



Merging New and Old Concepts: Tandem Oxidative Radical-Polar Crossover Ritter Amidation via Multicomponent Photo- and Electrochemical Processes

Mattia Lepori⁺,^[a] Indrasish Dey⁺,^[a] Cassie Pratley,^{*,[a]} and Joshua P. Barham^{*,[a, b]}

Dedicated to Profs. John A. Murphy and John C. Walton for their contributions to radical chemistry, including radical polar crossover.

Nitrogen-containing drug molecules and pharmaceuticals are ubiquitous, rendering the construction of C–N bonds a crucial target in methodology development. The Ritter reaction is a well-established method for accessing C–N bonds by generating amide functionality through the reaction of carbocations and nitriles. Since its discovery back in 1948, the Ritter reaction has progressively advanced towards milder and more sustainable conditions for carbocation generation. In this regard, notable contributions have been made by means

of single electron transfer (SET) chemistry. Nowadays, photo- and electrochemistry are established methods of choice for the generation of reactive radical intermediates and their subsequent oxidation *via* radical-polar crossover (RPC) mechanism. We review recent examples of tandem RPC and Ritter-type protocols, demonstrating how photo- and electrochemical energies have been effectively harvested to expand the precursor pool for the Ritter reaction as well as reimagining the process with novel mechanisms and additives.

1. Introduction

Given the pivotal role of amides in medicinal chemistry and drug discovery, the Ritter reaction is considered a notable milestone in synthetic organic chemistry.^[1,2] In the classical version reported by Ritter and co-workers in 1948,^[3,4] alcohols and alkenes are subjected to stoichiometric quantities of H₂SO₄ to generate their corresponding carbocations **1.1** (Scheme 1A). The latter is subsequently trapped by a nitrile, forming the nitrilium ion **1.2**, that is hydrolyzed to liberate the final amide product **1.3**. Although the process requires only readily available chemical feedstocks, the large quantity of acid needed precludes the use of sensitive functional groups. To effectively broaden the pool of precursors, numerous efforts have been undertaken over the years, as summarized in the evolutionary pathway depicted in Scheme 1A. The initial step towards developing a milder Ritter reaction involved employing catalytic amounts of Brønsted (e.g. H₂SO₄, *p*-TsOH, etc.)^[5,6] or Lewis acids (e.g. BF₃Et₂O, FeCl₃, etc.)^[7,8] Comprehensive reviews by Raymond and Cossy,^[9] as well as by Li and Zhang,^[10] describe how these advancements enabled the use of alkyl halides,^[11,12]

esters^[13,14] and epoxides^[15] as precursors in the so-called ‘non-classical’ Ritter process (*i.e.* Ritter-type).^[1] As described so far, the Ritter reaction has undergone extensive development using polar chemistry. However, the evolution of this model process owes much to the advent of radical chemistry, particularly radical-polar crossover (RPC).^[16–21] First introduced by Murphy in 1993^[22–24] and markedly advanced by MacMillan and Nicewicz in the early 2000s,^[25] the powerful concept of RPC offers a unique approach for combining the peculiar reactivity of radicals and ions in a one-pot manner. Specifically, once the radical intermediate is generated *via* single electron transfer (SET)^[26,27] or hydrogen atom transfer (HAT),^[28–31] it is converted into an ionic intermediate (a carbocation, in the context of this Review) *via* a subsequent SET event. Alternatively, the initially generated radical species is intercepted in tandem transformations (e.g. Giese additions) prior to RPC. In the case of reductive RPC to carbanions, it is more challenging to achieve difunctionalizations due to competitive protonation,^[32–34] so strong electrophiles (e.g. CO₂, aldehydes)^[17,35,36] or internal electrophiles are required.^[17,37,38] On the other hand, tandem radical addition/oxidative RPC provides a valuable, practicable platform for difunctionalizations *via* a diversity of nucleophiles, without requiring stringently dry conditions. This enables the incorporation of two distinct, orthogonal functionalities (e.g. into alkenes C–C double bonds, *vide infra*) in cascade processes.

Expanding on this powerful strategy to access carbocations, several new methods, described herein as tandem oxidative RPC Ritter-type amidations, have been developed. In fact, by leveraging SET and HAT chemistry, new precursors can be utilized. Additionally, various categories of reactions have been introduced, differing in how substrates are activated to generate the radical intermediate. In the first class, which will not be described in this Review, thermal processes are

[a] M. Lepori,⁺ I. Dey,⁺ Dr. C. Pratley, Dr. J. P. Barham
Fakultät für Chemie und Pharmazie, Universität Regensburg, Universitätsstraße 31, Regensburg 93040, Germany
E-mail: Cassie.Pratley@chemie.uni-regensburg.de
Joshua-Philipp.Barham@chemie.uni-regensburg.de

[b] Dr. J. P. Barham
University of Strathclyde, 295 Cathedral Street, Glasgow G1 1XL, UK

[⁺] These authors contributed equally.

© 2024 The Authors. European Journal of Organic Chemistry published by Wiley-VCH GmbH. This is an open access article under the terms of the Creative Commons Attribution License, which permits use, distribution and reproduction in any medium, provided the original work is properly cited.

employed to initiate radical formation. In this manner, both activated substrates like alkyl diacyl peroxides^[39] and α -aryl ketones,^[40] as well as non-activated substrates such as alkanes,^[41–43] can be engaged. Particularly noteworthy is the example from Baran and co-workers, demonstrating the activation of C(sp³)–H bonds using Zn(OTf)₂, CuBr₂ and Select-fluor™ as the catalytic system.^[44] Thermal approaches that facilitate the use of challenging starting materials such as alkanes require temperatures between 60 and 100 °C, which certainly represents a key area of improvement. In the realm of the evolution of Ritter processes toward milder conditions (room temperature, avoiding strong acids), the present Review aims to outline the latest developments in Ritter reactions facilitated by single electron processes. In particular, the most recent strategies will be classified into three categories that complement and expand upon thermal processes. The first two categories harvest traceless and green reagents such as photons and electrons, for photoredox catalysis (PRC)^[45–47] and synthetic organic electrochemistry (SOE), respectively.^[48,49] The third category utilizes photons *and* electrons by merging aspects of PRC and SOE together and is termed photoelectrochemistry (PEC).^[50–52] Although each of these techniques offers variations in the types of accessible substrates/products and the methods of activation, they tend to follow similar reactivity profiles, which are depicted in Scheme 1B. The general PRC approach (Scheme 1B-I) primarily focuses on SET activation of radical precursors by means of a photocatalyst

(PC) in its excited state. The resulting radical then adds to an alkene, and the process is completed with the oxidative RPC step, closing the photoredox cycle and regenerating the photocatalyst. Alternatively, certain PCs in their excited states can trigger the homolytic cleavage of a C(sp³)–H bond *via* direct HAT (Scheme 1B-II). When the role of the PC is to activate a hydrogen abstractor precursor (Y) *via* SET, this is referred to as indirect HAT.^[29] In contrast, SOE methods offer the advantage of generating radicals from substrates that can be efficiently oxidized at the anode, then subsequently deprotonated to form their radical counterparts (Scheme 1B-III). A further anodic oxidation (RPC) then yields the cation which goes on to perform the Ritter step. This is usually balanced by the reduction of protons at the cathode, producing H₂ gas as a by-product. The method of PEC follows reactivities analogous to Scheme 1B-I and -II, where activation of a substrate occurs by an excited state PC, followed by an oxidative RPC *via* an intermediate of the PC or the anode. Within this context, this review endeavors to summarize advantages, scalability, limitations and future perspectives of the chemistries, emphasizing the possibilities to further expand precursor pools and to explore new mechanisms for enhancing Ritter-type processes.



Mattia Lepori was born in 1998 in Pescia (Tuscany, Italy) and received his M.Sc. (cum laude) in Organic Chemistry at the University of Pisa in 2022. During his M.Sc., he worked on new cyclopentannulation strategies for the stereo-controlled synthesis of the isoprostanooids core under the supervision of Prof. Alessandro Mandoli. In late 2022, he joined the group of Dr. Joshua P. Barham at the University of Regensburg as a Ph.D candidate of the Elite Network of Bavaria's International Doctoral College 'Chemical Catalysis with Photonic or Electric Energy Input', where he investigates electro- and/or photochemical approaches for the synthesis of pharmaceutical and bioactive cores, including radical polar crossover reactions.



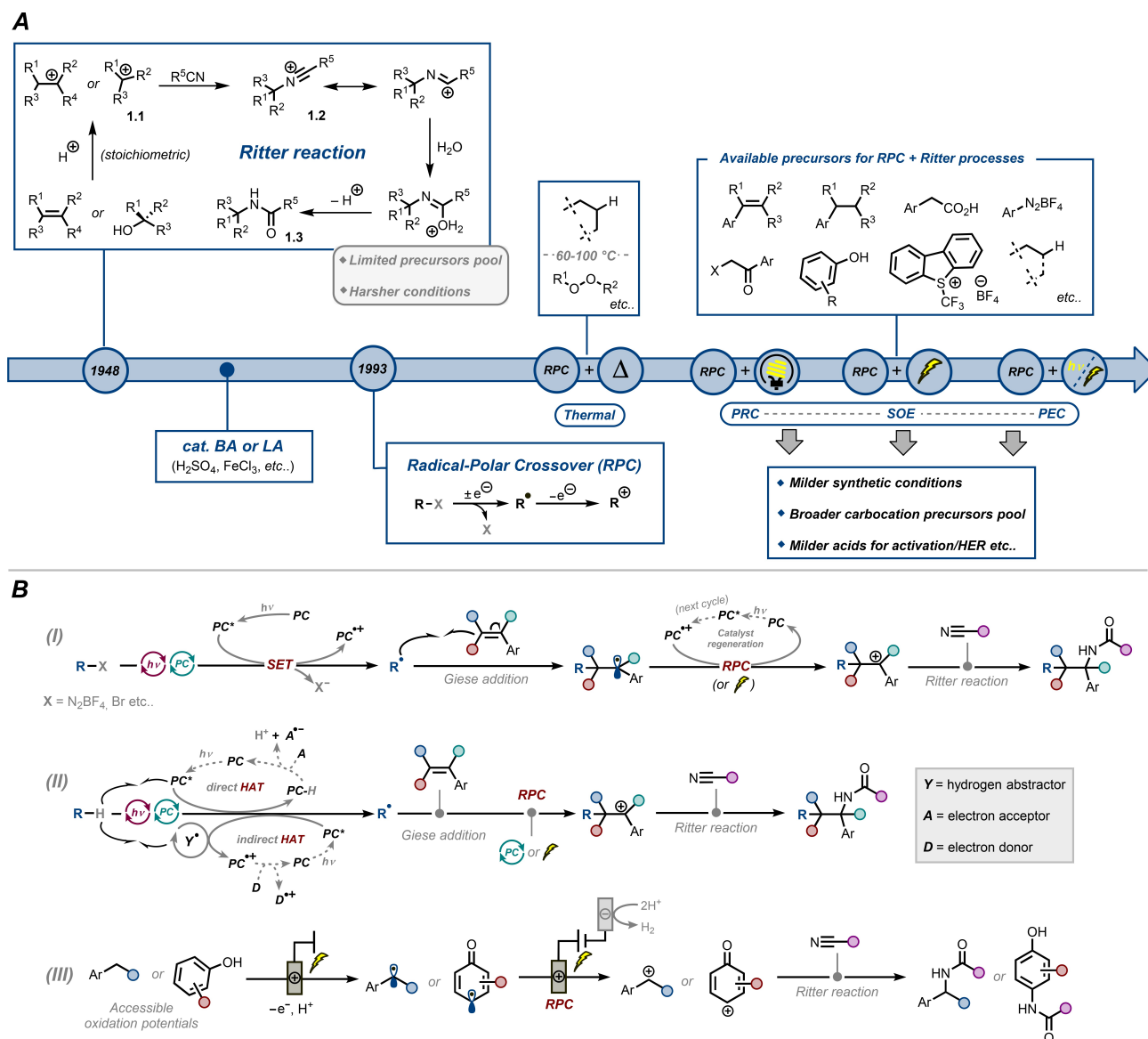
Indrasish Dey was born in Kolkata, India. He completed his B.Sc. in Chemistry at St. Stephen's College, University of Delhi, in 2022. During his undergraduate studies, he gained valuable research experience interning under the guidance of Dr. Chinmoy K. Hazra at the Indian Institute of Technology, Delhi. In 2022, he moved to Germany to pursue an M.Sc. in Advanced Synthesis and Catalysis as part of the Elite Network of Bavaria at the University of Regensburg. He completed his Master Thesis under the supervision of Dr. Joshua P. Barham. His research primarily focuses on visible light photoredox catalysis and synthetic photoelectrochemistry.



Cassie Pratley was born in Windsor, U.K. She completed her M.Chem. degree at the University of Bath in 2019, which included an industrial placement year at GSK, Stevenage, U.K. She received her industry-based Ph.D in 2023 under the supervision of Prof. John. A. Murphy and Dr. Sabine Fenner at the University of Strathclyde and GSK, U.K., where she investigated radical-mediated C–H amination methodologies and dynamically-mixed continuous flow reactions. In 2024, she joined the group of Dr. Joshua P. Barham at the University of Regensburg for postdoctoral research on synthetic photochemistry for post-modifications using gas-liquid flow reactors.



Joshua P. Barham was born in Watford, U.K. He received his industry-based Ph.D in 2017 under the supervision of Prof. John. A. Murphy and Dr. Matthew P. John at the University of Strathclyde and GSK, U.K. His postdoctoral studies in Japan with Prof. Yasuo Norikane (AIST) and Prof. Yoshitaka Hamashima (University of Shizuoka) specialized in flow chemistry and photoredox catalysis. His independent career started in 2019 at the University of Regensburg, supported by a Sofja Kovalevskaia Award, where his group investigates photo-, electro-, photoelectro- and continuous flow organic synthesis. In 2024, he was appointed Reader at the University of Strathclyde and Adjunct Professor at the University of Regensburg.

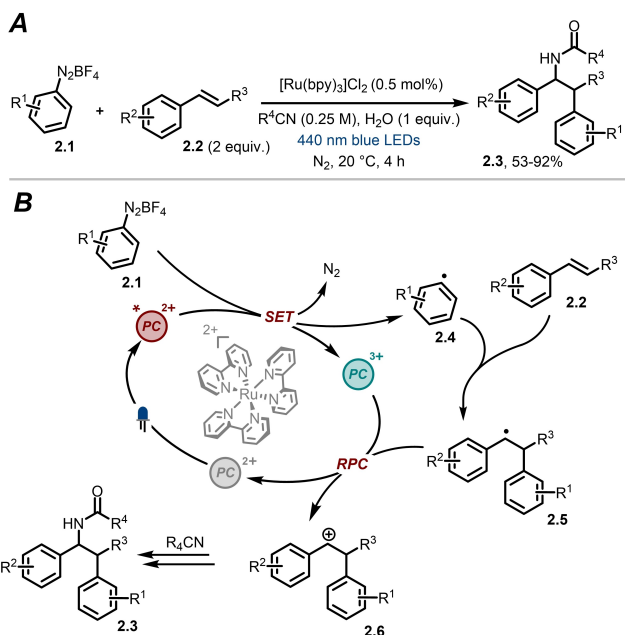


Scheme 1. A) Historical and methodological evolution of the Ritter reaction. B) General activation and reactivity modes for radical polar crossover processes mediated by photoredox catalysis, synthetic organic electrochemistry or photoelectrochemistry.

2. Photochemical Strategies

Visible light PRC has experienced a rapid surge in the last 20 years and has become an invaluable tool for synthetic organic chemists.^[45–47] PRC provides convenient methods to generate open-shell species under mild reaction conditions, which can be further utilized in several downstream processes. In this respect, radical difunctionalizations of olefins are a valuable addition to the synthetic chemist's toolbox, enabling rapid installation of two different functional groups across a double bond in a one-pot protocol.^[53–56] In fact, alkenes and their related analogues are ideal starting materials for constructing complex molecules due to their availability in bulk quantities from renewable resources and petrochemical feedstocks.^[57]

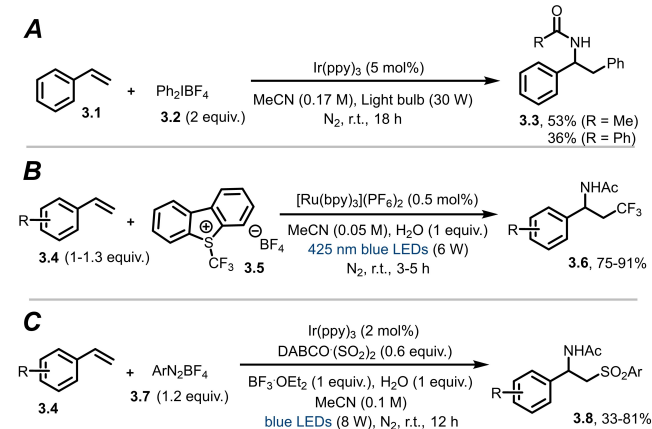
The first example of this transformation was reported by the König group in 2014, where photochemical amidoarylation of styrenes **2.2** was achieved by employing diazonium salts **2.1** via Meerwein-type additions,^[58] obtaining products **2.3** in good to excellent yields (53–92% in Scheme 2A).^[59] An initial oxidative quenching of the excited ruthenium (II)-based photocatalyst ($*E_{1/2} = -0.81$ V vs SCE)^[60] by **2.1** ($E_{1/2} = -0.16$ V vs SCE for R¹ = H)^[61,62] generates aryl radical **2.4** (Scheme 2B). Addition of the latter to **2.2** generates the intermediate **2.5**, which undergoes RPC to generate benzylic cation **2.6**. Finally, the cation is trapped *in situ* by a nitrile (R⁴CN) and undergoes a formal Ritter reaction in the presence of a stoichiometric amount of water to furnish the amidoarylated product **2.3**. The presence of a weakly nucleophilic counter-anion, tetrafluoroborate (BF₄⁻), is key to ensure selective attack of the carbocation by the nitrile, avoiding potential side reactions (*i.e.* hydroxyalkylation/elimination).



Scheme 2. A) Photoredox catalyzed amidoarylation of alkenes *via* Meerwein addition. B) Proposed mechanism.

nation). Diminishing the loading of nitrile from solvent equivalents to 10 equivalents (in dichloromethane) still achieves 70% yield of **2.3**. However, increasing the amount of water from 1 to 10 equivalents affords only a 42% yield of **2.3** and 1,2-diphenylethanol as a by-product. This demonstrates that a careful balance between the quantities of nitriles and water is crucial in these processes.

In addition to aryldiazonium salts, diaryliodonium salts allow facile generation of aryl radicals under mild photochemical settings. Greaney and co-workers exploited diaryliodonium salts **3.2** ($E_{1/2}$ = from -0.20 V to -0.36 V vs SCE)^[63,64] as aryl radical precursors and styrene **3.1** in a three-component reaction to synthesize amidoarylated products **3.3** (Scheme 3A).^[65] In a

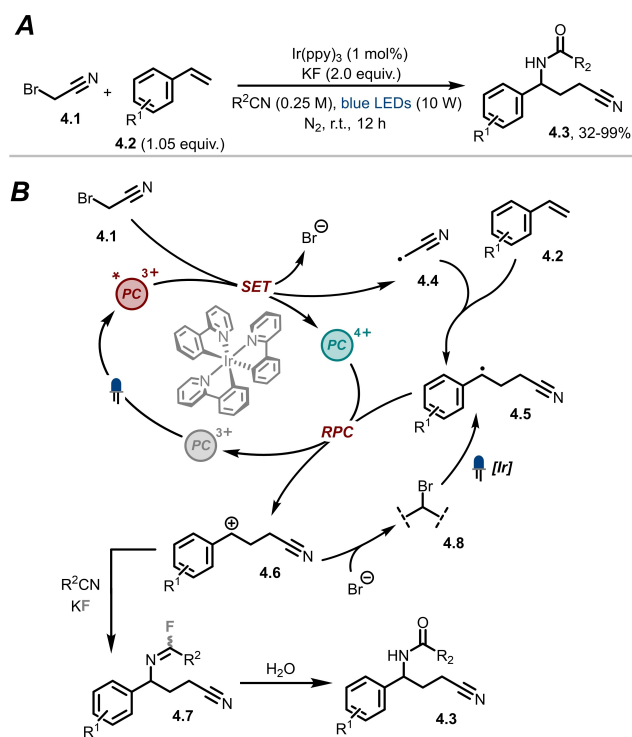


Scheme 3. A) Photoredox catalyzed amidoarylation of alkenes. B) Photoredox catalyzed amidotrifluoromethylation of alkenes. C) Photoredox catalyzed amidosulfonylation of alkenes.

related example, Umemoto's reagent **3.5** ($E_{1/2}$ = -0.72 V vs SCE)^[66,67] was harnessed by Koike, Akita and co-workers as a trifluoromethyl radical source for aminotrifluoromethylation^[68] of alkenes to furnish the corresponding products **3.6** in high to excellent yields (75–91%, Scheme 3B).^[69]

Moreover, given the importance of sulfonyl groups in pharmaceutical molecules,^[70,71] a multicomponent route towards β -sulfonyl amides **3.8** was developed by the Wu group (Scheme 3C).^[72] In this report, the authors utilized 1,4-diazabicyclo[2.2.2]octane bis(sulfur dioxide) adduct [DABCO(SO₂)₂] as a sulfur dioxide source^[73] and aryldiazonium salt **3.7** as an aryl radical precursor, which combine to generate an arylsulfonyl radical intermediate. The latter undergoes radical addition followed by RPC (*cf.* Scheme 2B) and Ritter-type reaction to generate the product **3.8**. As in previous examples, the use of solvent-equivalent amounts of nitrile was required to overcome competitive undesired addition of water.

As seen so far, in a classical Ritter reaction the role of water is indispensable in hydrolysis of the nitrilium intermediate to release the amide product. For this reason, additives that promote the hydrolysis step are desirable to maximize product formation yields. In this regard, the Chen group reported an elegant photochemical three-component Ritter-type reaction of styrenes **4.2** with alkyl bromides **4.1** as radical sources, facilitated by potassium fluoride (KF) as a pivotal additive (Scheme 4A).^[74] Mechanistically, the reaction proceeds with an initial SET reduction of α -bromoacetonitrile **4.1** ($E_{1/2}$ = -0.69 V vs SCE)^[75] by the excited state of the iridium (III)-based photocatalyst ($^*E_{1/2}$ = -1.73 V vs SCE)^[60] to generate α -cyano radical intermediate **4.4** (Scheme 4B). The latter engages in a Giese-



Scheme 4. A) Photoredox catalyzed alkylamidation of alkenes *via* α -bromo nitrile activation. B) Proposed mechanism.

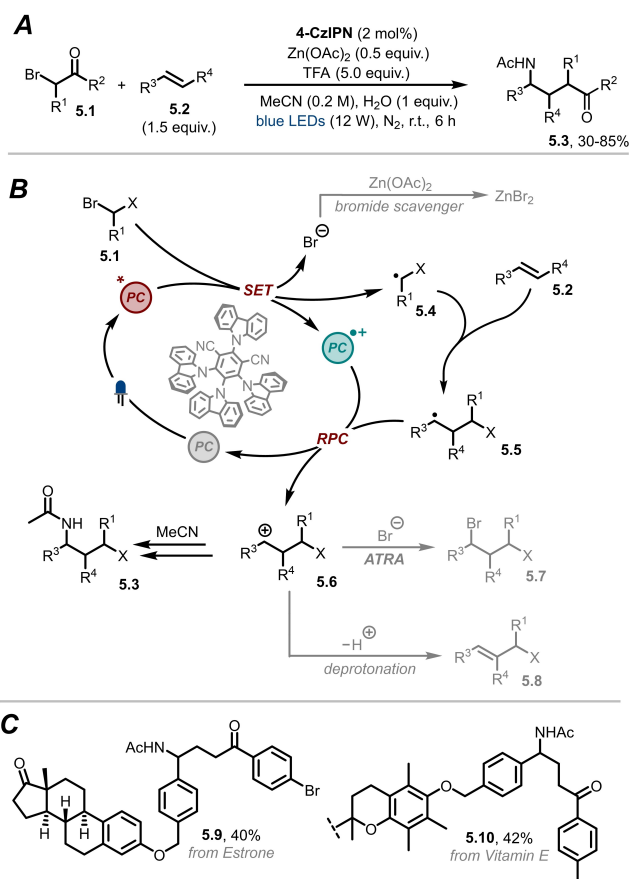
type radical addition to **4.2**, furnishing benzylic radical **4.5**. This is subsequently converted to the corresponding cation **4.6** via RPC, regenerating the photocatalyst ground state. At this stage, **4.6** is attacked by the nitrile (R^2CN) to generate the nitrilium ion transiently, which is efficiently trapped by fluoride ion (from KF) to furnish the imidoyl fluoride intermediate **4.7**. Finally, the latter undergoes hydrolysis to yield the products **4.3** in modest to excellent yields (32–99%).

However, the facilitation of the hydrolysis step is not the only role attributed to KF by the authors. In fact, while halo-derivatives such as **4.1** are economical and readily accessible radical sources, their most important limitation lies in the formation of bromide during the activation stage. This results in the highly atom-economical atom transfer radical addition (ATRA) carbobromination products (e.g. **4.8** in Scheme 4B).^[76,77] During the optimization study, the authors noted that when KF was not present, bromide **4.8** was obtained in 70% yield and **4.3** was not detected. On the other hand, no ATRA product was detected when KF was added, indicating that the additive plays a decisive role in directing the trapping of the intermediate, to regulate product selectivity. Within the mechanistic rationalization, it has also been proposed that even if generated, **4.8** can revert to intermediate **4.5** through photoredox pathways.

Building on the previous results, Maity and co-workers harvested α -bromo ketones **5.1** as radical precursors in a $Zn(OAc)_2$ promoted alkylamidation of alkenes, including both styrenes and aliphatic olefins (Scheme 5A).^[78] The mechanism resembles the one described in Scheme 4B. In particular, the reaction starts with the SET reduction of **5.1** by the excited state of the organophotocatalyst 1,2,3,5-tetrakis (carbazol-9-yl)-4,6-dicyanobenzene (**4-CzIPN**, $E_{1/2}^* = -1.18$ V vs SCE)^[79] to generate the α -keto radical **5.4**. The latter undergoes radical addition to olefin **5.2** to produce intermediate **5.5**. Upon the formation of **5.6**, a Ritter-type reaction occurs, furnishing product **5.3** (Scheme 5B).

The $Zn(OAc)_2$ additive plays a crucial role in scavenging bromide ions from the reaction medium and suppressing ATRA by-product **5.7**. This resulted in the generation of $ZnBr_2$, as confirmed by the authors through energy dispersive X-ray (EDX) analysis of the evaporated aqueous phase. Given the high reduction potential of **5.1** (e.g. $E_{1/2} = -1.45$ V vs SCE for 2-bromoacetophenone),^[80] the second consistent role of the Lewis acidic zinc salt involves enhancing the reactivity of alkyl halide substrate **5.1**. This is probably achieved by metal coordination to the ketone moiety's oxygen atom, thereby lowering the reduction potential of the carbonyl group to single electron reduction. Interestingly, the Heck-type coupling product **5.8**, that could result from a competitive deprotonation from **5.6** was also suppressed under the optimized reaction conditions. Finally, regarding the substrate scope, the authors successfully difunctionalized a variety of complex alkenes derived from pharmaceuticals such as Estrone (**5.9**) and Vitamin E (**5.10**), thereby demonstrating the important synergy of Late Stage Functionalization (LSF)^[81,82] and Ritter-type processes (Scheme 5C).

The previous examples of Ritter-type amidations required redox-active functionalities to facilitate the initial generation of

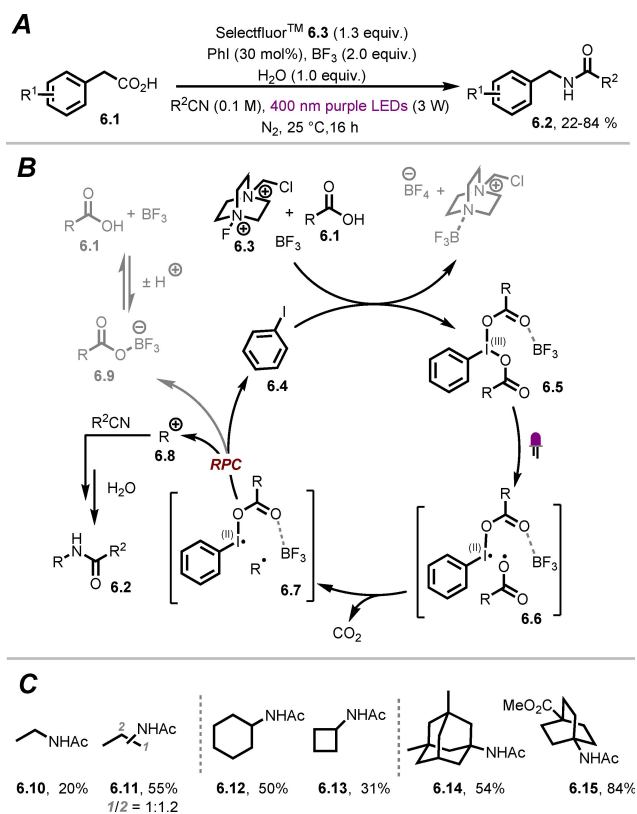


Scheme 5. A) Photoredox catalyzed alkylamidation of alkenes via α -halo ketone or ester activation. B) Proposed mechanism. C) Substrate scope.

a carbon-centred radical. However, such pre-functionalized starting materials limit the utility of synthetic protocols. For this reason, more accessible, abundant, cost-effective and non-toxic cationic precursors are desirable. Carboxylic acids, which represent abundant and widely used feedstocks in synthetic organic chemistry, meet these criteria.^[57]

König and co-workers reported a photocatalyst-free decarboxylative amidation of benzylic carboxylic acids **6.1**, harnessing the ability of *in situ* generated iodine(III)- BF_3 complex to absorb visible light (Scheme 6A).^[83] The authors were able to synthesize the corresponding amidated product **6.2** using catalytic amounts of iodobenzene, stoichiometric SelectfluorTM **6.3** as terminal oxidant and BF_3 as Lewis acid, along with MeCN as the nitrile source and a stoichiometric amount of water.

In the mechanism, iodobenzene **6.4** is firstly oxidized by SelectfluorTM to generate a hypervalent iodine(III) species, which in presence of carboxylic acid **6.1** and BF_3 gives rise to the visible light absorbing complex **6.5** (Scheme 6B). At this stage, BF_3 also helps in scavenging oxidation by-products of **6.3**. Irradiation of **6.5** with a 400 nm light source enabled the homolytic scission of the I–O bond to transiently form the carboxyl radical in an intermediate akin to **6.6**. Subsequent decarboxylation generates the radical (R^*), which is subsequently oxidized by the iodine-centred radical species in **6.7**, leading to the cation (R^+ , **6.8**). Nitrile trapping and Ritter-type



Scheme 6. A) Decarboxylative Ritter-type amidation *via* excitation of *in situ* generated iodine (III)-BF₃ complex. B) Proposed mechanism. C) Example scope.

reaction releases the amidated products **6.2** in poor to very good yields (22–84%). The regenerated iodobenzene **6.4** can further restart the catalytic cycle. In the same manner, **6.1** and BF₃ are released following the decomplexation of **6.9**.

Remarkably, difficult to engage non-benzylic aliphatic carboxylic acids were also competent under a slightly modified protocol, where 2 equivalents of **6.3** and a catalytic amount of I₂ were added. This facilitated the decarboxylation to non-stabilized species such as primary radicals. With the optimized conditions in hand, both primary (**6.10** and **6.11**) and secondary (**6.12** and **6.13**) carboxylic acids were functionalized. Tertiary acids were also employed, accessing interesting motifs such as memantine and an unnatural amino acid building block (**6.14** and **6.15**, respectively) (Scheme 6C).

An equivalent approach was published by the same group for the functionalization of benzylic C(sp³)–H bonds.^[84] In this area, activation of C(sp³)–H bonds *via* HAT provides an elegant, direct access to carbon-centred radicals.^[28–31] Benzylic and tertiary C(sp³)–H bonds are particularly privileged owing to their accessible bond dissociation energies (BDE ≈ 88 kcal/mol for toluene and ≈ 96 kcal/mol for isobutane).^[29] The mechanism of action reported by König and co-workers is analogous to the iodine(I/III) cycle just described (*cf.* Scheme 6B, where a HAT process occurs instead of decarboxylation).

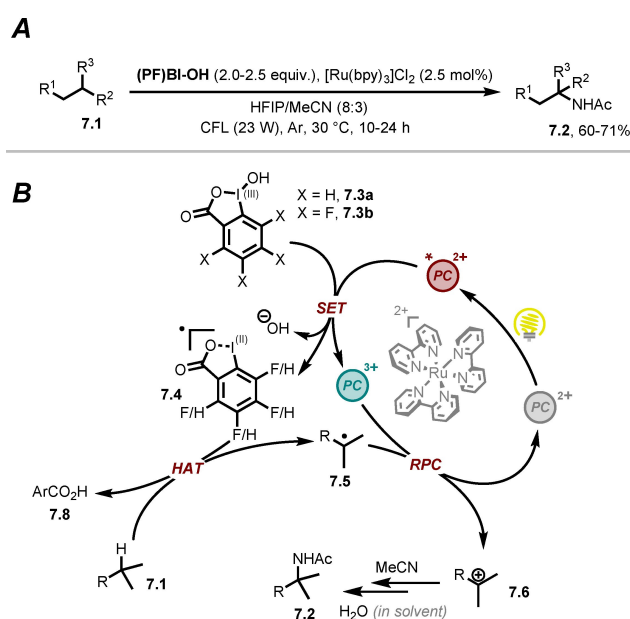
In the realm of hypervalent iodine chemistry, Chen and co-workers reported an efficient protocol for the acetamidation of

benzylic and tertiary C–H bonds (**7.1**). This employed hydroxyl benziodoxole **BI-OH** (**7.3a** for benzylic C–H bonds) or the pentafluoro equivalent **PFBI-OH** (**7.3b** for tertiary C–H bonds) and a ruthenium (II)-based photocatalyst, producing the corresponding products **7.2** in good yields (60–71%, Scheme 7A).^[85]

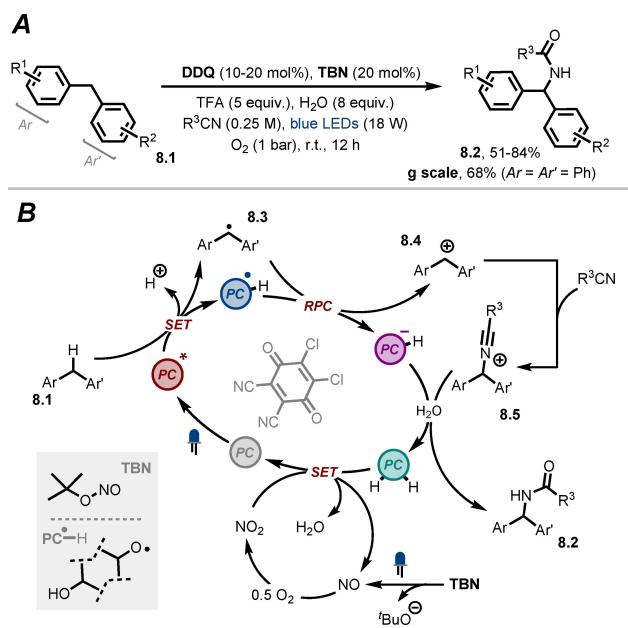
Regarding the mechanistic rationalization, (PF)BI-OH (**7.3**) is reduced by the excited state of [Ru(bpy)₃]Cl₂ to generate (perfluoro)benziodoxole radical **7.4** (Scheme 7B). The latter can participate in HAT with **7.1** to yield the corresponding benzylic or tertiary radical **7.5** with high regioselectivity and the aryl carboxylic acid **7.8** as a by-product. The RPC event generates carbocation **7.6** and regenerates the photocatalyst, as per a classical redox-neutral process. A formal Ritter process occurs via water present in the solvent mixture and the acetamide product **7.2** is released.

Finally, the group of Shen and co-workers developed a photocatalytic aerobic benzylic C–H amidation reaction under ambient conditions. In presence of catalytic amounts of 2,3-dichloro-5,6-dicyano-1,4-benzoquinone (DDQ), *tert*-butyl nitrite (TBN) and stoichiometric molecular oxygen (1 bar) as a green oxidant, the authors successfully amidated benzylic C–H bonds of diarylmethanes **8.1** (BDE ≈ 84 kcal/mol for diphenylmethane), accessing products **8.2** in good to very good yields (51–84%, Scheme 8A).^[86] The significance of certain quantities of additives like H₂O and TFA was highlighted in these examples through the use of control reactions, demonstrating again their pivotal role in obtaining high yields in Ritter-type processes. The reaction was scalable in batch, with successful execution at a gram scale (6 mmol) resulting in a 68% yield when diphenylmethane (Ar = Ar' = Ph) was employed as a substrate.

In the mechanism, irradiation of ground state DDQ with blue light generates the triplet excited state *DDQ (*E_{1/2} = +3.18 V vs SCE).^[87] This engages **8.1** *via* consecutive SET



Scheme 7. A) Photoredox catalyzed C(sp³)–H bonds amidation (using hypervalent iodine). B) Proposed mechanism.



Scheme 8. A) Photoredox catalyzed aerobic Ritter-type C(sp³)–H bond amidation. B) Proposed mechanism.

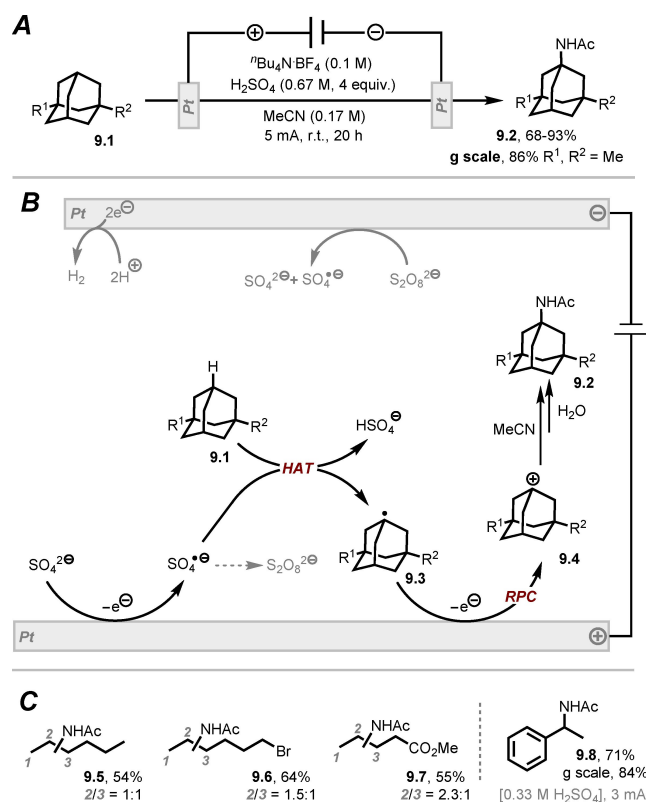
oxidation and proton transfer to generate stabilized radical **8.3** (Scheme 8B). Subsequently, the mono-hydrogenated radical form of the catalyst, DDQH[•], oxidizes the latter to yield the corresponding cation **8.4**, in the RPC event, resulting in the formation of the mono-hydrogenated anion catalyst species, DDQH[–]. Nucleophilic attack of the reaction solvent R³CN to **8.4** leads to the corresponding nitrilium ion **8.5**, which is hydrolyzed in presence of H₂O and TFA to furnish the amidated product **8.2**. Regarding the catalyst's fate, DDQH[–] is protonated during the hydrolysis step to form DDQH₂. Finally, the latter is oxidized to regenerate DDQ by NO₂, which is produced *in situ* via aerobic oxidation of NO, in turn liberated through photolysis of TBN.

3. Electrochemical Strategies

The earliest synergy between electrochemically-mediated RPC reactions and the Ritter reaction dates back to the 1970's. The groups of Pletcher,^[88] Miller,^[89–92] Mayeda^[93] and co-workers were pioneers in utilizing electrons as traceless reagents for the functionalization of C(sp³)–H bonds under potentiostatic conditions (*i.e.* constant potential electrolysis) with platinum-based anodes. In this manner, Ritter-type amidations were performed starting from alcohols,^[93] esters,^[89] ketones,^[90,94] and even alkanes^[88] such as adamantane.^[92] For the latter, initial anodic oxidation leads to the corresponding tertiary radical *via* proton loss, and the subsequent oxidation event generates the carbocation, which can react with nitriles to yield the corresponding acetamide. Despite the lack of useful experimental details (*e.g.* counter electrode material),^[95,96] along with the high anodic potentials required, these seminal works reflect the ability of electrochemistry to engage substrates, both activated

and non-activated, to obtain amidated derivatives. Building on these encouraging premises, various tandem RPC and Ritter-type strategies have been developed in recent years, contributing to what is coined as a “Renaissance” of SOE in the 2000s.^[48,49,97]

Given the importance of amine derivatives of adamantanes (*e.g.* memantine) in the treatment of Alzheimer's disease,^[98,99] and inspired by Miller's early report,^[92] Ma, Ye and co-workers reported an elegant and green method for the functionalization of adamantanes (Scheme 9A).^[100] In particular, unlike direct anodic oxidation, **9.1** was activated *via* HAT^[29] with the sulfate radical anion SO₄^{•–}, the latter of which can be electrochemically generated through anodic oxidation of a sulfate anion (SO₄^{2–}) or cathodic reduction of a peroxydisulfate dianion (S₂O₈^{2–}). In this manner, different adamantanes were functionalized, yielding products **9.2** in good to excellent yields (68–93%) under galvanostatic conditions (*i.e.* constant current electrolysis) in an undivided cell setup. Utilizing an affordable source of sulfate like H₂SO₄ in acetonitrile, the authors were able to scale up the batch process up to a gram scale (10 mmol). Regarding the mechanism, once anodically generated, SO₄^{•–} abstracts a hydrogen from the most electron-rich C(sp³)–H bond that leads to the most stabilized radical. For **9.1**, tertiary radical **9.3** is generated (Scheme 9B). The latter is oxidized at the anode in the RPC event to yield the carbocation **9.4**, that is trapped by acetonitrile, the reaction solvent. A classical Ritter process is mediated by the water present in H₂SO₄, or by the NaHCO₃

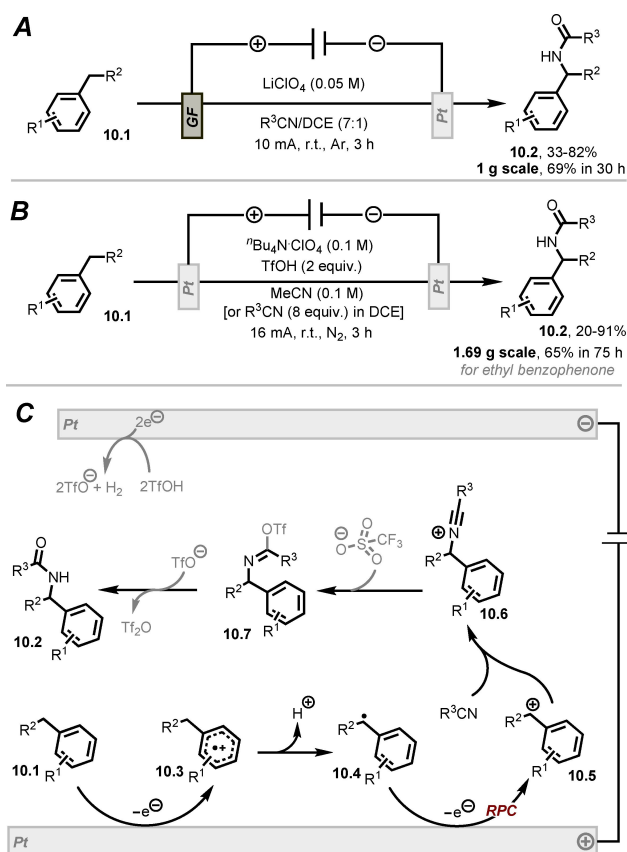


Scheme 9. A) Electrochemical Ritter-type amidation of C(sp³)–H bonds *via* hydrogen atom transfer. B) Proposed mechanism. C) Example scope. Pt = platinum electrode.

saturated solution used for the work-up, liberating the amidated product **9.2**. Furthermore, the authors efficiently expanded the scope of the process to linear alkanes such as *n*-hexane (**9.5**, Scheme 9C). In this manner, mixtures of regioisomers were obtained, with a selectivity bias toward the C(sp³)–H bond that leads to a secondary radical and that is furthest from the electron withdrawing group (**9.6** and **9.7**).

Finally, easily activated alkylbenzene substrates (BDE ≈ 84 kcal/mol for benzylic C(sp³)–H bonds vs ≈ 95 kcal/mol for tertiary and ≈ 98 kcal/mol for secondary C(sp³)–H bonds)^[29,101] were successfully employed for the syntheses of **9.8** and analogues thereof in both milligram and gram scales. In these cases, the concentration of H₂SO₄ was adjusted to 0.33 M and the current was decreased from 5 mA to 3 mA.

Functionalization of benzylic C(sp³)–H positions is a popular route to synthesise bioactive and pharmaceutical motifs.^[102,103] Other research groups have focused on developing methods that obviate the need for metal catalysts or chemical oxidants. Recently, two similar undivided cell procedures achieved direct anodic oxidation of alkylarenes, such as **10.1**, to generate acetamidated products **10.2** (Scheme 10A and Scheme 10B).^[104,105] The groups of Liu, Sun and the group of Zhou successfully employed both acetonitrile and various nitriles (R³CN), achieving gram scale reactions in batch with good yields (69% and 65%, respectively).



Scheme 10. A) Electrochemical Ritter-type amidation of benzylic C(sp³)–H bonds by Liu, Sun and co-workers. B) Electrochemical Ritter-type amidation of benzylic C(sp³)–H bonds by Zhou and co-workers. C) Proposed mechanism by Zhou and co-workers. GF = graphite electrode.

In the mechanism, the two protocols share the same initial oxidation phase. In particular, anodic oxidation of alkylarenes **10.1** ($E_{1/2} = +1.89$ V vs SCE for 4-ethyl-1,1'-biphenyl and $E_{1/2} = +2.59$ V vs SCE for 1-(4-ethylphenyl)ethan-1-one)^[104] yields their radical cations **10.3** (Scheme 10C). Deprotonation of the latter leads to a benzylic radical **10.4**, that is further oxidized at the anode in the RPC event to generate carbocation **10.5** for the last step. Upon obtaining the iminium ion **10.6**, the two procedures diverge in the concluding stages of the Ritter-type process, particularly concerning the identity of the nucleophile responsible for liberating product **10.2**. In this regard, Liu, Sun and co-workers conducted an isotopic labelling experiment adding 2 equivalents of H₂¹⁸O. The ¹⁸O-marked product **10.2** was detected by HRMS, confirming that water is hydrolyzing **10.6**, as per a classical Ritter mechanism (*cf.* Scheme 1A). Since no explicit amount of water is added under the standard conditions, it can be hypothesized that the water present in the solvent or supporting electrolyte (*i.e.* LiClO₄ is highly hygroscopic), along with the aqueous workup, completes the process.

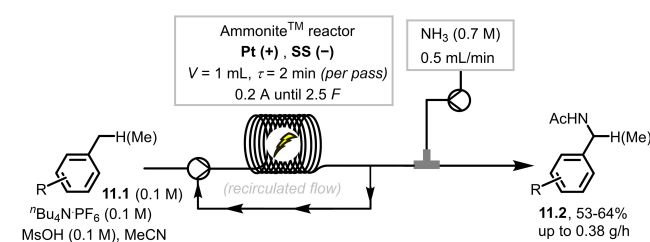
More interesting is the dual role of triflic acid (TfOH) demonstrated by Zhou and co-workers. The primary function involves supplying stoichiometric quantities of protons. In fact, it is well established that a counter-reaction is crucial in electrochemistry to facilitate electron flow through the cell.^[106,107] For oxidation processes, the most common counter-reaction is the hydrogen evolution reaction (HER),^[96,108] consisting of proton source reduction at the cathodic surface. As for the first example (Scheme 10A), while there does not appear to be a clear proton source, protons released in the formation of **10.4** must be sufficient for this purpose. Finally, regarding the second role of TfOH proposed by Zhou and co-workers,^[103] the conjugated base of the acid (triflate, TfO⁻) reacts with **10.6** to yield the intermediate **10.7**. The Ritter-type product **10.2** is finally obtained *via* a detrifluoromethanesulfonylation reaction, liberating triflic anhydride (Tf₂O) as a by-product, that was detected by GC-MS.

The recent growth of SOE has been accelerated by the utilization of cutting-edge reactor platform technologies. In this context, continuous flow chemistry has emerged as a powerful platform for scalable, reproducible and efficient (in terms of Faradaic efficiency) electrochemical reactions in both academic and industrial settings.^[109,110] Electrochemical continuous flow reactors offer important advantages over batch scale-up. Among the most relevant, these include: *i)* the narrowing of the interelectrode distance, which consequently decreases the cell resistance and mitigates the need for a large quantity of supporting electrolyte; *ii)* the minimized risk of over-oxidation (or reduction) of target products due to the shorter residence times inside the reactor; *iii)* in cases involving gas formation (*e.g.* H₂), the coalescence of gas bubbles in microreactors generally enhances performances thanks to an increased mass transfer, while in batch gas bubbles forming on the electrode surface can give rise to zones of low conductivity, causing heat buildup and decreased efficiency.^[111,112]

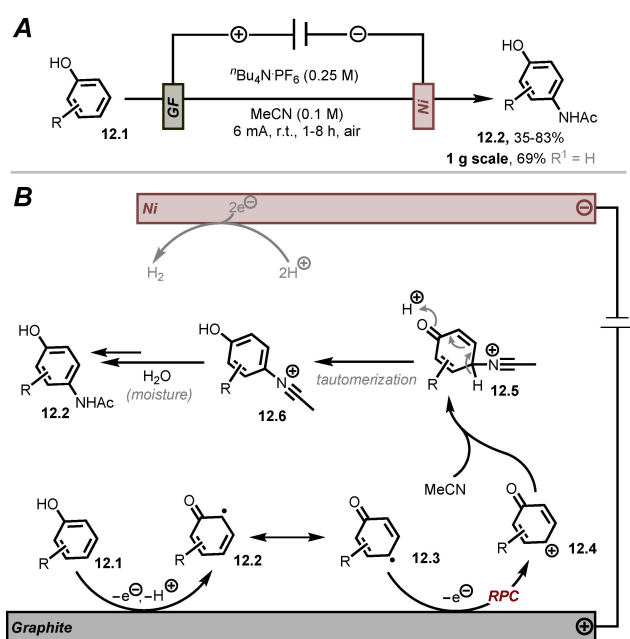
In this regard, Ley and co-workers disclosed a continuous flow protocol for the amidation of C(sp³)–H benzylic bonds employing a 1 mL Ammonite™ reactor.^[113] Harvesting electro-

chemical energy, the authors functionalized alkylarenes like **11.1**, obtaining the corresponding products **11.2** in good yields (53–63%) and with productivities up to 0.38 g/h (Scheme 11).^[114] In their setup, the solution of **11.1**, supporting electrolyte and methanesulfonic acid (MsOH) in MeCN was continuously pumped through the reactor with a flow rate of 0.5 mL/min (a corresponding residence time (τ) of 2 minutes per pass), recirculating for around 9 h. To avoid decomposition of **11.2** under acidic conditions, the outlet flux was mixed with a pumped basic solution of NH₃ in MeOH.

In addition to the previously discussed C(sp³)–H bond activation, the functionalization of C(sp²)–H bonds constitutes a field of considerable significance.^[115] Within this area, the arylamine (or amide) moiety is among the most prevalent motifs in organic synthesis, that appears in a plethora of bioactive and pharmaceutically-relevant substances.^[116] Given this importance, different pathways have been developed for the formation of C(sp²)–N bonds. Classical strategies (*e.g.* Buchwald-Hartwig cross-coupling, Chan-Lam oxidative coupling, *etc.*),^[117,118] involve the use of preactivated substrates and require high temperatures, precious metal catalysts and stoichiometric chemical oxidants. Electrochemistry offers a



Scheme 11. Continuous flow electrochemical Ritter-type amidation of C(sp³)–H bonds. SS = stainless steel electrode.



Scheme 12. A) Electrochemical Ritter-type C–H amidation of phenols. B) Proposed mechanism. Ni = nickel electrode.

milder and greener approach to functionalizing arenes by means of direct C(sp²)–H activation. In this context, the first promising evidences for tandem electrochemically-mediated RPC and Ritter reactions were reported by Miller^[91] and Parker^[119] in the 1970's for the acetamidation of aromatic carbonyl compounds (*e.g.* acetophenone) at the *para*- and *ortho*- positions and anthracenes at the C(9)-position. Inspired by these findings, Banerjee and co-workers reported a regioselective electrochemical Ritter-type amidation of phenols **12.1** (Scheme 12A).^[120] With an undivided cell setup, the authors were able to synthesize acetyl-*para*-aminophenol derivatives **12.2** (commonly known as paracetamol when R = H) using constant current electrolysis in acceptable to high yields (35–83%).

In contrast to classical reported syntheses (*e.g.* Hoechst-Celanese route),^[121] that require multiple steps, the authors were able to obtain paracetamol in a fast single step requiring only 1–8 hours. Additionally, the procedure proved to be scalable in batch up to gram scale, yielding the active pharmaceutical ingredient in 69% yield. Regarding the mechanism, the reaction starts with the anodic oxidation of the phenol **12.1** ($E_{1/2} = +1.63$ vs SCE for R = H)^[122] to afford the α -keto radical **12.3** after proton release (Scheme 12B). After that, the γ -keto radical species **12.3** forms and subsequent radical polar crossover affords the carbocation **12.4**. Despite not being clearly defined, according to the authors, the *para*-selectivity could be driven by a sum of polar and steric effects. Addition of acetonitrile to **12.4** affords the nitrilium ion **12.5**, that tautomerizes to intermediate **12.6**. Finally, water from moisture hydrolyses the latter, releasing the Ritter-type product **12.2**.

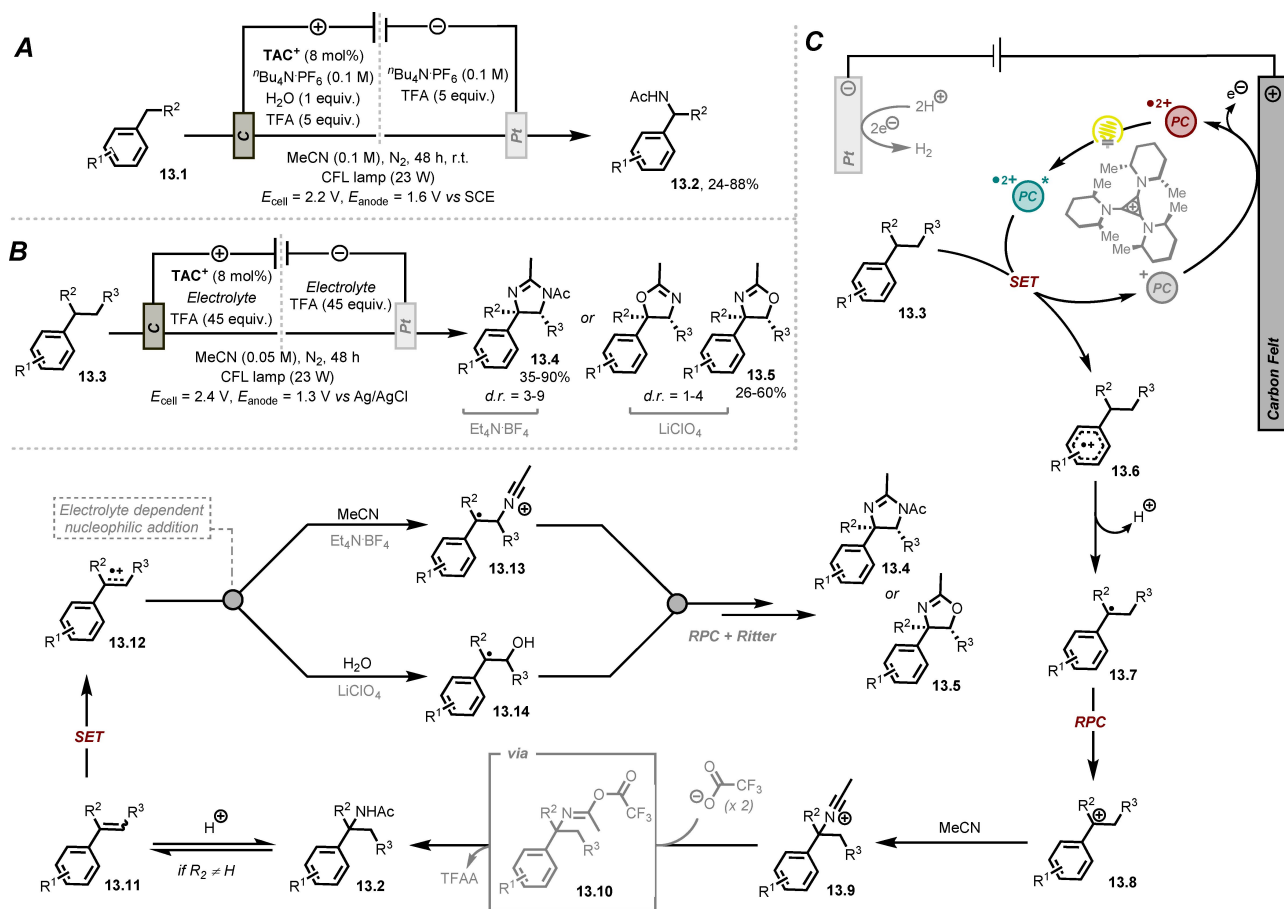
4. Photoelectrochemical Strategies

Rapid advancements in photochemistry and electrochemistry have markedly propelled the generation of radical intermediates forward. Nevertheless, each field comes with its limitations.^[123] For instance, PRC is constrained by the limited range of substrates it can engage and the necessity for stoichiometric oxidants (or reductants) for net-redox processes. For SOE, challenges such as over-oxidation (or reduction) and electrode passivation persist due to the high potentials applied. Combining these two methodologies has effectively overcome their limitations, leading to the development of synthetic photoelectrochemistry (PEC).^[50–52] PEC encompasses various subclasses, relevant to this Review is electrochemically-mediated photoredox catalysis (*e*-PRC),^[124,125] in which the electrochemical and photochemical steps are present in the same catalytic cycle as consecutive events. This further divides into: *i*) Radical ion *e*-PRC, where electrogenerated radical ions are photoexcited to generate super-oxidants or super-reductants; *ii*) Recycling *e*-PRC, where the turnover of the classical photoredox catalyst occurs through anodic oxidation or cathodic reduction.

Under photoelectrochemical conditions, Lambert and co-workers reported a C–H Ritter-type monoamidation of unbranched alkylarenes **13.1**. In particular, the synergy between trisaminocyclopropenium ion (TAC⁺) pre-photocatalyst and

potentiostatic conditions in a divided cell setup successfully yielded functionalized products **13.2** in poor to very good yields (24–88%, Scheme 13A).^[126] Interestingly, by simply adjusting the conditions and starting from α -branched alkylarenes **13.3**, the same group described an efficient divergent photoelectrochemical synthesis of dihydroimidazoles **13.4**^[127] or oxazolines **13.5**,^[128] depending on the electrolyte used (Scheme 13B).^[129] In the mechanism, the two processes share the same initial phase. **TAC**⁺ ($E_{1/2} = +1.26$ V vs SCE) is electrochemically oxidized at the anode to generate the dication radical **TAC**^{•2+}. Photoexcitation of the latter leads to the superoxidant species ***TAC**^{•2+} ($*E_{1/2} = +3.33$ V vs SCE), as per a radical cation e-PRC process. The active catalyst then engages **13.3** in a single electron transfer oxidation, generating the radical cation **13.6**, which liberates the benzylic radical **13.7** upon proton release (Scheme 13C). Regarding the first step, since the anodic potential is not sufficient to engage **13.3** ($E_{\text{anode}} = 1.6$ V vs $E_{1/2}$ from +1.8 to +2.5 V vs SCE for alkylarenes, cf. discussion of Scheme 10C), the authors claimed that the oxidation is mediated by the electro-activated photocatalyst. Since products **13.2** have similar oxidation potentials to the starting materials, this leads to a minimized risk of overoxidation of target molecules compared to pure electrochemical conditions. After the RPC step for **13.7**, carried out by **TAC**^{•2+} or the anode,

acetonitrile nucleophilically attacks **13.8** and leads to the nitrilium ion **13.9**. At this point, the authors propose that the hydrolysis step might proceed *via* nucleophilic attack by the trifluoroacetate ion, forming the trifluoroacetimidate **13.10**. This species can then undergo deacylation to yield Ritter-type product **13.2** and trifluoroacetic anhydride (TFAA) as a by-product (cf. Scheme 10C for a similar role of triflate). Upon the formation of the monoamidated species, the reaction stops if the starting material is an unbranched alkylarene (*i.e.* $R^2 = \text{H}$ in Scheme 13C). Alternatively, when $R^2 = \text{alkyl}$ or aryl, **13.2** experiences a reversible, acid-catalyzed E_1 elimination to yield the styrene **13.11**. This selectivity can be attributed to the greater tendency of α -branched species to undergo elimination even in the presence of trifluoroacetic acid (TFA), whereas non-branched species require notably stronger acids (*e.g.* TfOH). At this stage, **13.11** undergoes oxidation to generate the radical cation **13.12**, which then participates in the supporting electrolyte-dependent step. Specifically, when Et_4NBF_4 is employed, nucleophilic addition of acetonitrile produces the intermediate **13.13**. However, with LiClO_4 as an additive, **13.14** is formed by the attack of water present in the hygroscopic salt. Although not expanded on by the authors, the divergent nature of this step can be explained by the nature of the electrolyte's anion, that guides divergent reactivity with acetonitrile or water.



Scheme 13. A) Photoelectrochemical Ritter-type amidation of benzylic C(sp³)-H bonds. B) Photoelectrochemical diamidation of α -branched alkyl arenes. C) Proposed mechanism for both processes.

Finally, further oxidations of the radical intermediates and subsequent intramolecular Ritter-type processes release the cyclized products **13.4** and **13.5**.

Building on the promising protocol to access oxindoles starting from alkylarenes, Lambert and co-workers extended the photoelectrochemical method to aryl olefins **14.1** to give rise to **14.2** (Scheme 14A).^[130] In particular, the significance of these building blocks lies in the fact that aryl-substituted 1,2-aminoalcohols play essential roles as structural motifs in diverse complex molecules, including natural compounds^[131] and chiral ligands.^[132] The sole distinction from the preceding protocols resides in the explicit addition of an excess of water (5 equivalents), while **TAC**⁺ serves as the electro-activated photocatalyst and TFA once again serves to supply protons for the counter HER reduction.

Regarding the mechanism, upon generation of ***TAC**²⁺ (cf. Scheme 13C), the latter oxidatively engages **14.1** ($E_{1/2}$ from $\approx +1.15$ to $\approx +1.95$ V vs SCE)^[122] to afford the corresponding radical cation **14.3** (Scheme 14B). Nucleophilic attack by water leads to radical intermediate **14.4**, that can be further oxidized in the RPC step by **TAC**²⁺ or at the anode surface to generate benzylic cation **14.5**. Finally, nitrilium ion **14.6** formation and an intramolecular Ritter-type process from the alcohol moiety releases the oxindole derivative **14.2**. The photoelectrochemical approach in this case represents a notable advancement over electrochemistry alone, allowing selective engagement of olefins without associated risks of overoxidation.

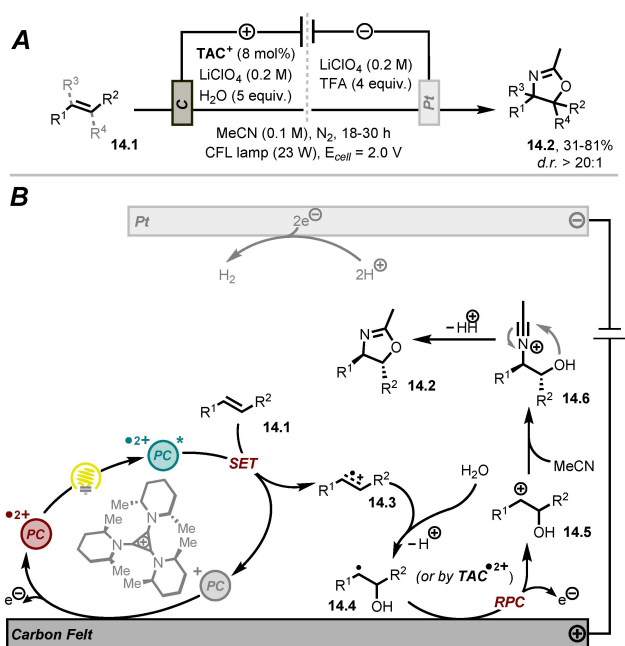
Tian, Barham and co-workers recently reported a divided cell photoelectrochemical approach to difunctionalize styrenes **15.2**, leveraging HAT and starting from inexpensive and abundant unactivated alkanes **15.1**. In this manner, carboamidated products **15.3** were obtained in poor to good yields (19–

65%) using tetra-*n*-butylammonium decatungstate (**TBADT**, (*n*-Bu₄N)₄[W₁₀O₃₂]) as the photocatalyst (Scheme 15A).^[133]

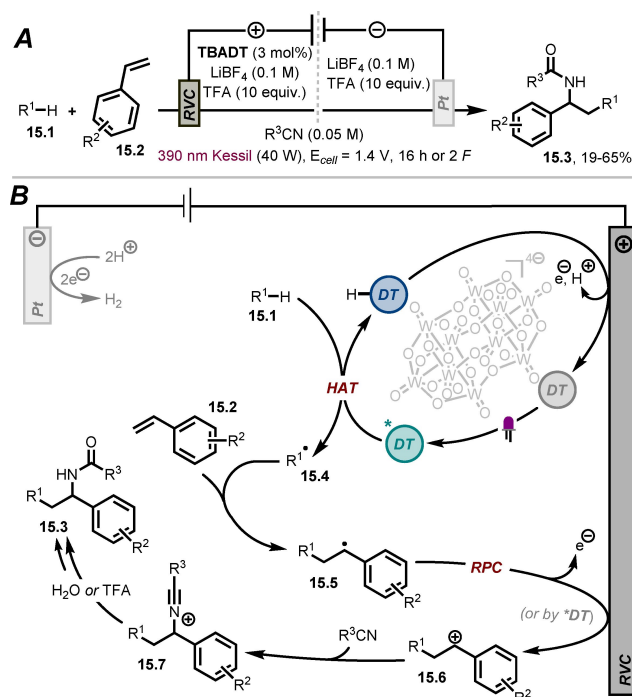
In the mechanism, irradiation of the latter with purple light generates its excited state ***TBADT**, which engages the C(sp³)–H bonds of substrates **15.1** *via* HAT to generate the corresponding alkyl radicals **15.4** (Scheme 15B). Giese-type addition of the radical to the styrene **15.2** leads to the benzylic radical intermediate **15.5**, that is further oxidized by the anode or by ***TBADT** ($E_{1/2} = +2.44$ vs SCE)^[134] to generate cation **15.6**. Solvent trapping yields the nitrilium ion **15.7**, that can be hydrolyzed by the water present in the electrolyte (or provided in the aqueous workup) or stepwise *via* the trifluoroacetate-trapped intermediate (cf. Scheme 13C). Regarding the catalyst's regeneration, the reduced form **TBADT-H** undergoes anodic oxidation and deprotonation in an overall recycling *e*-PRC process.

5. Summary and Outlook

This Review summarizes the most recent developments in the field of Ritter-type amidation reactions using oxidative RPC approaches (from 2010 to present) under photo- and/or electrochemical conditions. In particular, the importance of the synergy between radical and polar chemistry in achieving reactions under milder conditions was highlighted, thereby broadening the precursor pool far beyond alcohols and alkenes initially reported by Ritter and co-workers in 1948.^[3,4] As discussed above, both activated and non-activated radical precursors can now be efficiently engaged harvesting SET



Scheme 14. A) Photoelectrochemical amidooxygenation of aryl olefins. B) Proposed mechanism.



Scheme 15. A) Photoelectrochemical carboamidation of alkenes. B) Proposed mechanism. RVC = reticulated vitreous carbon electrode, DT = decatungstate.

chemistry without the need for high temperatures and harsh conditions (e.g. the use of stoichiometric amounts of strong acids). On the other hand, tandem RPC-Ritter-type methods offer the synthetic community a salient opportunity to difunctionalize alkenes (*vide supra*) with two distinct and orthogonal functional groups in a one-pot manner, eliminating the need to isolate intermediates.

Finally, it is necessary to highlight that certain areas of improvement undoubtedly remain. Among these, it is worth mentioning: *i*) the need for more methodologies that can exploit highly reactive species such as primary radicals for efficient syntheses in useful yields; *ii*) the need to cut down on large excesses of nitriles needed (often as solvent) to out-compete undesired reactions, which may be achievable through trapping incipient radicals with catalytic metal complexes that can serve as carbocation equivalents,^[135] *iii*) the potential to scale up the presented methods to an industrial level, for instance, by utilizing cutting-edge technologies such as flow reactors. We hope that this Review will further stimulate interest in developing the concept of RPC-Ritter-type processes, utilizing novel radical precursors and technologies. Moreover, we aim to foster a better understanding of the mechanisms involved and elucidate the roles certain additives play in the nitrilium ion hydrolysis step (e.g. TFA or TfOH) to release the desired amidated compounds.

Acknowledgements

M. L. and J. P. B. are members of the Elite Network of Bavaria (ENB) International Doctoral College: "IDK Chemical Catalysis with Photonic or Electric Energy Input" and M. L. is grateful to the ENB for financial support. I.D. is grateful for funding provided by the University of Regensburg and the SynCat programme of the ENB. C. P. and J. P. B. acknowledge funding provided by the Alexander von Humboldt Foundation within the framework of the Sofja Kovalevskaja Award endowed by the German Federal Ministry of Education and Research to J. P. B. Open Access funding enabled and organized by Projekt DEAL.

Conflict of Interests

The authors declare no conflicts of interest.

Data Availability Statement

Data sharing is not applicable to this article as no new data were created or analyzed in this study.

Keywords: Amination · Radical polar crossover · Single electron transfer · Ritter reaction · Amidation

[1] D. Jiang, T. He, L. Ma, Z. Wang, *RSC Adv.* **2014**, *4*, 64936–64946.

- [2] G. Mohammadi Ziarani, F. Soltani Hasankiadeh, F. Mohajer, *Chemistry-Select* **2020**, *5*, 14349–14379.
- [3] J. J. Ritter, P. P. Minieri, *J. Am. Chem. Soc.* **1948**, *70*, 4045–4048.
- [4] J. J. Ritter, J. Kalish, *J. Am. Chem. Soc.* **1948**, *70*, 4048–4050.
- [5] D. Desnelli, *Macromol. Symp.* **2015**, *353*, 198–204.
- [6] M. Nasr-Esfahani, M. Montazerzohori, Z. Karami, *Org. Prep. Proced. Int.* **2016**, *48*, 321–327.
- [7] H. Firouzabadi, A. R. Sardarian, H. Badparva, *Synth. Commun.* **1994**, *24*, 601–607.
- [8] R. I. Khusnutdinov, T. M. Egorova, R. I. Aminov, Y. Y. Mayakova, E. S. Mescheryakova, *Synth. Commun.* **2020**, *50*, 564–570.
- [9] A. Guérinot, S. Reymond, J. Cossy, *Eur. J. Org. Chem.* **2012**, *2012*, 19–28.
- [10] M.-E. Chen, X.-W. Chen, Y.-H. Hu, R. Ye, J.-W. Lv, B. Li, F.-M. Zhang, *Org. Chem. Front.* **2021**, *8*, 4623–4664.
- [11] R. Leiva, S. Gazzarrini, R. Esplugas, A. Moroni, L. Naesens, F. X. Sureda, S. Vázquez, *Tetrahedron Lett.* **2015**, *56*, 1272–1275.
- [12] T. Bykova, N. Al-Maharik, A. M. Z. Slawin, M. Bühl, T. Lebl, D. O'Hagan, *Chem.-Eur. J.* **2018**, *24*, 13290–13296.
- [13] H. Hamadi, Z. Zanjani, M. Yadollahi, *Polyhedron* **2020**, *175*, 114219.
- [14] C.-L. Feng, B. Yan, M. Zhang, J.-Q. Chen, M. Ji, *Chem. Pap.* **2019**, *73*, 535–542.
- [15] C. N. Rao, F. A. Khan, *Org. Biomol. Chem.* **2015**, *13*, 2768–2775.
- [16] *The Radical Polar Crossover Reaction*, J. A. Murphy in *Radicals Organic Synthesis* (Eds.: P. Renaud, M. P. Sibi), Wiley-VCH Verlag GmbH, Weinheim, **2001**; ch. 2.7, pp. 298–315.
- [17] L. Pitzer, J. L. Schwarz, F. Glorius, *Chem. Sci.* **2019**, *10*, 8285–8291.
- [18] S. Sharma, J. Singh, A. Sharma, *Adv. Synth. Catal.* **2021**, *363*, 3146–3169.
- [19] M. Liu, X. Ouyang, C. Xuan, C. Shu, *Org. Chem. Front.* **2024**, *11*, 895–915.
- [20] Z. Tan, H. Zhang, K. Xu, C. Zeng, *Sci. China Chem.* **2024**, *67*, 450–470.
- [21] R. J. Wiles, G. A. Molander, *Isr. J. Chem.* **2020**, *60*, 281–293.
- [22] C. Lampard, J. A. Murphy, N. Lewis, *J. Chem. Soc., Chem. Commun.* **1993**, (3), 295–297.
- [23] J. A. Murphy, F. Rasheed, S. Gastaldi, T. Ravishanker, N. Lewis, *J. Chem. Soc., Perkin Trans. 1* **1997**, *1*, 1549–1558.
- [24] J. A. Murphy, F. Rasheed, S. J. Roome, K. A. Scott, N. Lewis, *J. Chem. Soc., Perkin Trans. 1* **1998**, *1*, 2331–2340.
- [25] D. A. Nicewicz, D. W. C. MacMillan, *Science* **2008**, *322*, 77–80.
- [26] E. C. Ashby, *Acc. Chem. Res.* **1988**, *21*, 414–421.
- [27] M. P. Plesniak, H. M. Huang, D. J. Procter, *Nat. Rev. Chem.* **2017**, *1*, 1–16.
- [28] L. Capaldo, D. Ravelli, *Eur. J. Org. Chem.* **2017**, *2017*, 2056–2071.
- [29] L. Capaldo, D. Ravelli, M. Fagnoni, *Chem. Rev.* **2022**, *122*, 1875–1924.
- [30] L. Chang, S. Wang, Q. An, L. Liu, H. Wang, Y. Li, K. Feng, Z. Zuo, *Chem. Sci.* **2023**, *14*, 6841–6859.
- [31] F. S. Meger, J. A. Murphy, *Molecules* **2023**, *28*, 6127.
- [32] T. Wan, L. Capaldo, G. Laudadio, A. V. Nyuchev, J. A. Rincón, P. García-Losada, C. Mateos, M. O. Frederick, M. Nuño, T. Noël, *Angew. Chem., Int. Ed.* **2021**, *60*, 17893–17897.
- [33] X. Tian, T. A. Karl, S. Reiter, S. Yakubov, R. de Vivie-Riedle, B. König, J. P. Barham, *Angew. Chem., Int. Ed.* **2021**, *60*, 20817–20825.
- [34] B.-C. Hong, R. R. Indurmuddam, *Org. Biomol. Chem.* **2024**, *22*, 3799–3842.
- [35] K. Donabauer, B. König, *Acc. Chem. Res.* **2021**, *54*, 242–252.
- [36] W. Zhang, S. Lin, *J. Am. Chem. Soc.* **2020**, *142*, 20661–20670.
- [37] J. P. Phelan, S. B. Lang, J. S. Compton, C. B. Kelly, R. Dykstra, O. Gutierrez, G. A. Molander, *J. Am. Chem. Soc.* **2018**, *140*, 8037–8047.
- [38] C. Shu, R. S. Mega, B. J. Andreassen, A. Noble, V. K. Aggarwal, *Angew. Chem., Int. Ed.* **2018**, *130*, 15656–15660.
- [39] B. Qian, S. Chen, T. Wang, X. Zhang, H. Bao, *J. Am. Chem. Soc.* **2017**, *139*, 13076–13082.
- [40] M.-E. Chen, Z.-Y. Gan, Y.-H. Hu, F.-M. Zhang, *J. Org. Chem.* **2023**, *88*, 3954–3964.
- [41] S. Sakaguchi, T. Hirabayashi, Y. Ishii, *Chem. Commun.* **2002**, *2*, 516–517.
- [42] K. Kiyokawa, K. Takemoto, S. Minakata, *Chem. Commun.* **2016**, *52*, 13082–13085.
- [43] S. Liu, M. Klusmann, *Org. Chem. Front.* **2021**, *8*, 2932–2938.
- [44] Q. Michaudel, D. Thevenet, P. S. Baran, *J. Am. Chem. Soc.* **2012**, *134*, 2547–2550.
- [45] D. Ravelli, D. Dondi, M. Fagnoni, A. Albini, *Chem. Soc. Rev.* **2009**, *38*, 1999.
- [46] C. K. Prier, D. A. Rankic, D. W. C. MacMillan, *Chem. Rev.* **2013**, *113*, 5322–5363.

- [47] L. Marzo, S. K. Pagire, O. Reiser, B. König, *Angew. Chem., Int. Ed.* **2018**, *57*, 10034–10072.
- [48] E. J. Horn, B. R. Rosen, P. S. Baran, *ACS Cent. Sci.* **2016**, *2*, 302–308.
- [49] M. Yan, Y. Kawamata, P. S. Baran, *Chem. Rev.* **2017**, *117*, 13230–13319.
- [50] J. P. Barham, B. König, *Angew. Chem., Int. Ed.* **2020**, *59*, 11732–11747.
- [51] H. Huang, K. A. Steiniger, T. H. Lambert, *J. Am. Chem. Soc.* **2022**, *144*, 12567–12583.
- [52] L. Qian, M. Shi, *Chem. Commun.* **2023**, *59*, 3487–3506.
- [53] X. Lan, N. Wang, Y. Xing, *Eur. J. Org. Chem.* **2017**, *2017*, 5821–5851.
- [54] M. Patel, B. Desai, A. Sheth, B. Z. Dholakiya, T. Naveen, *Asian J. Org. Chem.* **2021**, *10*, 3201–3232.
- [55] X. Bao, J. Li, W. Jiang, C. Huo, *Synthesis* **2019**, *51*, 4507–4530.
- [56] Y. Liu, H. Liu, X. Liu, Z. Chen, *Catalysts* **2023**, *13*, 1056.
- [57] A. Marshall, P. J. Alaimo, *Chem.-Eur. J.* **2010**, *16*, 4970–4980.
- [58] N. Diesendorf, M. R. Heinrich, *Synthesis* **2022**, *54*, 1951–1963.
- [59] D. P. Hari, T. Hering, B. König, *Angew. Chem., Int. Ed.* **2014**, *53*, 725–728.
- [60] *Photoredox Catalysis of Iridium(III)-Based Photosensitizers*, T. M. Monos, C. R. J. Stephenson in *Iridium(III) Optoelectron. Photonics Applications* (Ed.: E. Zysman-Colman), Wiley-VCH Verlag GmbH, Weinheim, **2017**, pp. 541–581.
- [61] C. P. Andrieux, J. Pinson, *J. Am. Chem. Soc.* **2003**, *125*, 14801–14806.
- [62] F. Mo, D. Qiu, L. Zhang, J. Wang, *Chem. Rev.* **2021**, *121*, 5741–5829.
- [63] J. L. Dektar, N. P. Hacker, *J. Org. Chem.* **1990**, *55*, 639–647.
- [64] J. Lalevée, N. Blanchard, M. Tehfe, M. Peter, F. Morlet-Savary, J. P. Fouassier, *Macromol. Rapid Commun.* **2011**, *32*, 917–920.
- [65] G. Fumagalli, S. Boyd, M. F. Greaney, *Org. Lett.* **2013**, *15*, 4398–4401.
- [66] S. Mizuta, S. Verhoog, X. Wang, N. Shibata, V. Gouverneur, M. Médebielle, *J. Fluor. Chem.* **2013**, *155*, 124–131.
- [67] C. Zhang, *Org. Biomol. Chem.* **2014**, *12*, 6580.
- [68] Z. Wang, J.-H. Lin, J.-C. Xiao, *Org. Lett.* **2024**, *26*, 1980–1984.
- [69] Y. Yasu, T. Koike, M. Akita, *Org. Lett.* **2013**, *15*, 2136–2139.
- [70] X. Chen, S. Hussain, S. Parveen, S. Zhang, Y. Yang, C. Zhu, *Curr. Med. Chem.* **2012**, *19*, 3578–3604.
- [71] F. Zhao, J. Wang, X. Ding, S. Shu, H. Liu, *Chinese J. Org. Chem.* **2016**, *36*, 490.
- [72] Y. Zong, Y. Lang, M. Yang, X. Li, X. Fan, J. Wu, *Org. Lett.* **2019**, *21*, 1935–1938.
- [73] H. Woolven, C. González-Rodríguez, I. Marco, A. L. Thompson, M. C. Willis, *Org. Lett.* **2011**, *13*, 4876–4878.
- [74] Y.-Q. Guan, X.-T. Min, G.-C. He, D.-W. Ji, S.-Y. Guo, Y.-C. Hu, Q.-A. Chen, *iScience* **2021**, *24*, 102969.
- [75] A. A. Isse, A. Gennaro, *J. Phys. Chem. A* **2004**, *108*, 4180–4186.
- [76] T. Courant, G. Masson, *J. Org. Chem.* **2016**, *81*, 6945–6952.
- [77] S. Engl, O. Reiser, *Chem. Soc. Rev.* **2022**, *51*, 5287–5299.
- [78] A. Samanta, S. Pramanik, S. Mondal, S. Maity, *Chem. Commun.* **2022**, *58*, 8400–8403.
- [79] E. Speckmeier, T. G. Fischer, K. Zeitler, *J. Am. Chem. Soc.* **2018**, *140*, 15353–15365.
- [80] E. Speckmeier, P. J. W. Fuchs, K. Zeitler, *Chem. Sci.* **2018**, *9*, 7096–7103.
- [81] T. Cernak, K. D. Dykstra, S. Tyagarajan, P. Vachal, S. W. Kraska, *Chem. Soc. Rev.* **2016**, *45*, 546–576.
- [82] R. Cannalire, S. Pelliccia, L. Sancineto, E. Novellino, G. C. Tron, M. Giustiniano, *Chem. Soc. Rev.* **2021**, *50*, 766–897.
- [83] R. Narobe, K. Murugesan, S. Schmid, B. König, *ACS Catal.* **2022**, *12*, 809–817.
- [84] R. Narobe, K. Murugesan, C. Haag, T. E. Schirmer, B. König, *Chem. Commun.* **2022**, *58*, 8778–8781.
- [85] G.-X. Li, C. A. Morales-Rivera, F. Gao, Y. Wang, G. He, P. Liu, G. Chen, *Chem. Sci.* **2017**, *8*, 7180–7185.
- [86] T. Li, J. Yang, X. Yin, J. Shi, Q. Cao, M. Hu, X. Xu, M. Li, Z. Shen, *Org. Biomol. Chem.* **2022**, *20*, 8756–8760.
- [87] M. T. Huynh, C. W. Anson, A. C. Cavell, S. S. Stahl, S. Hammes-Schiffer, *J. Am. Chem. Soc.* **2016**, *138*, 15903–15910.
- [88] D. B. Clark, M. Fleischmann, D. Pletcher, *J. Chem. Soc., Perkin Trans. 2* **1973**, (11), 1578.
- [89] L. L. Miller, V. Ramachandran, *J. Org. Chem.* **1974**, *39*, 369–372.
- [90] J. Y. Becker, L. R. Byrd, L. L. Miller, Y.-H. So, *J. Am. Chem. Soc.* **1975**, *97*, 853–856.
- [91] Y.-H. So, J. Y. Becker, L. L. Miller, *J. Chem. Soc., Chem. Commun.* **1975**, (7), 262.
- [92] V. R. Koch, L. L. Miller, *J. Am. Chem. Soc.* **1973**, *95*, 8631–8637.
- [93] E. A. Mayeda, *J. Am. Chem. Soc.* **1975**, *97*, 4012–4015.
- [94] J. Y. Becker, L. L. Miller, T. M. Siegel, *J. Am. Chem. Soc.* **1975**, *97*, 849–853.
- [95] D. M. Heard, A. J. J. Lennox, *Angew. Chem., Int. Ed.* **2020**, *59*, 18866–18884.
- [96] M. Klein, S. R. Waldvogel, *Angew. Chem., Int. Ed.* **2022**, *61*, 1–17.
- [97] Concurrently to this Review, a general overview of electrochemical Ritter-type transformations was published by the Ye group. Y. Ma, C. Liu, D. Yang, Z. Fang, W. Huang, R. Cheng, J. Ye, *Org. Biomol. Chem.* **2024**, *22*, 9766–9771.
- [98] G. Marotta, F. Basagni, M. Rosini, A. Minarini, *Molecules* **2020**, *25*, 4005.
- [99] S. Dragomanova, M. Lazarova, A. Munkuev, E. Suslov, K. Volcho, N. Salakhutdinov, A. Bibi, J. Reynisson, E. Tzvetanova, A. Alexandrova, A. Georgieva, D. Uzunova, M. Stefanova, R. Kalfin, L. Tancheva, *Molecules* **2022**, *27*, 5456.
- [100] L. Zhang, Y. Fu, Y. Shen, C. Liu, M. Sun, R. Cheng, W. Zhu, X. Qian, Y. Ma, J. Ye, *Nat. Commun.* **2022**, *13*, 4138.
- [101] L. Bering, S. Manna, A. P. Antonchick, *Chem.-Eur. J.* **2017**, *23*, 10936–10946.
- [102] N. A. McGrath, M. Brichacek, J. T. Njardarson, *J. Chem. Educ.* **2010**, *87*, 1348–1349.
- [103] U. Gulati, R. Gandhi, J. K. Laha, *Chem. Asian J.* **2020**, *15*, 3135–3161.
- [104] Q. Chu, Y. Zhou, C. Ji, P. Liu, P. Sun, *Synthesis* **2023**, *55*, 2969–2978.
- [105] Y. Xu, Q. Li, R. Ye, B. Xu, X. Zhou, *J. Org. Chem.* **2023**, *88*, 9518–9522.
- [106] J. E. Nutting, J. B. Gerken, A. G. Stamoulis, D. L. Bruns, S. S. Stahl, *J. Org. Chem.* **2021**, *86*, 15875–15885.
- [107] C. Schotten, T. P. Nicholls, R. A. Bourne, N. Kapur, B. N. Nguyen, C. E. Willans, *Green Chem.* **2020**, *22*, 3358–3375.
- [108] Y. Zheng, Y. Jiao, M. Jaroniec, S. Z. Qiao, *Angew. Chem., Int. Ed.* **2015**, *54*, 52–65.
- [109] K. Watts, A. Baker, T. Wirth, *J. Flow Chem.* **2014**, *4*, 2–11.
- [110] L. Capaldo, Z. Wen, T. Noël, *Chem. Sci.* **2023**, *14*, 4230–4247.
- [111] M. B. Plutschack, B. Pieber, K. Gilmore, P. H. Seeberger, *Chem. Rev.* **2017**, *117*, 11796–11893.
- [112] T. Noël, Y. Cao, G. Laudadio, *Acc. Chem. Res.* **2019**, *52*, 2858–2869.
- [113] Further information about the reactor can be found at <http://www.cambridgereactordesign.com/ammonite/ammonite.html> (accessed on 12.03.2024).
- [114] M. A. Kabeshov, B. Musio, S. V. Ley, *React. Chem. Eng.* **2017**, *2*, 822–825.
- [115] H. M. L. Davies, D. Morton, *J. Org. Chem.* **2016**, *81*, 343–350.
- [116] D. G. Brown, J. Boström, *J. Med. Chem.* **2016**, *59*, 4443–4458.
- [117] B. Seifinoferest, A. Tanbakouchian, B. Larjani, M. Mahdavi, *Asian J. Org. Chem.* **2021**, *10*, 1319–1344.
- [118] M. J. West, J. W. B. Fyfe, J. C. Vantourout, A. J. B. Watson, *Chem. Rev.* **2019**, *119*, 12491–12523.
- [119] O. Hammerich, V. D. Parker, *J. Chem. Soc. Chem. Commun.* **1974**, *3*, 245.
- [120] I. M. Taily, D. Saha, P. Banerjee, *Org. Lett.* **2022**, *24*, 2310–2314.
- [121] J. A. Berson, D. M. McDaniel, L. R. Corwin, J. H. Davis, *J. Am. Chem. Soc.* **1972**, *94*, 5508–5509.
- [122] H. Roth, N. Romero, D. Nicewicz, *Synlett* **2015**, *27*, 714–723.
- [123] N. E. S. Tay, D. Lehnerr, T. Rovis, *Chem. Rev.* **2022**, *122*, 2487–2649.
- [124] S. Wu, J. Kaur, T. A. Karl, X. Tian, J. P. Barham, *Angew. Chem., Int. Ed.* **2022**, *61*, e202107811.
- [125] M. Lepori, S. Schmid, J. P. Barham, *Beilstein J. Org. Chem.* **2023**, *19*, 1055–1145.
- [126] T. Shen, T. H. Lambert, *J. Am. Chem. Soc.* **2021**, *143*, 8597–8602.
- [127] M. Hossain, A. Nanda, *Sci. J. Chem.* **2018**, *6*, 83.
- [128] K. T. Ibrahim, M. Neetha, G. Anilkumar, *Monatsh. Chem.* **2022**, *153*, 837–871.
- [129] T. Shen, T. H. Lambert, *Science* **2021**, *371*, 620–626.
- [130] H. Huang, T. H. Lambert, *J. Am. Chem. Soc.* **2022**, *144*, 18803–18809.
- [131] E. Abraham, S. G. Davies, N. L. Millican, R. L. Nicholson, P. M. Roberts, A. D. Smith, *Org. Biomol. Chem.* **2008**, *6*, 1655.
- [132] G. Desimoni, G. Faita, K. A. Jørgensen, *Chem. Rev.* **2006**, *106*, 3561–3651.
- [133] S. Schmid, S. Wu, I. Dey, M. Domański, X. Tian, J. P. Barham, *ACS Catal.* **2024**, *14*, 9648–9654.
- [134] V. De Waele, O. Poizat, M. Fagnoni, A. Bagno, D. Ravelli, *ACS Catal.* **2016**, *6*, 7174–7182.
- [135] D. S. Chung, S. H. Park, S. Lee, H. Kim, *Chem. Sci.* **2021**, *12*, 5892–5897.

Manuscript received: July 25, 2024

Revised manuscript received: September 17, 2024

Accepted manuscript online: September 18, 2024

Version of record online: December 4, 2024